TÜBİTAK

**Turkish Journal of Earth Sciences**

**http://journals.tubitak.gov.tr/earth/**

**Research Article**

Turkish J Earth Sci
(2015) 24: 289-301

doi:10.3906/yer-1410-13

# Spatial-temporal analysis of seismicity before the 2012 Varzeghan, Iran, Mw 6.5 earthquake

**Mohammad TALEBI, Mehdi ZARE*, Rohollah MADAHI-ZADEH, Aref BALI-LASHAK**
Seismological Research Center, International Institute of Earthquake Engineering and Seismology, Tehran, Iran

**Received:** 20.10.2014 • **Accepted/Published Online:** 18.03.2015 • **Printed:** 29.05.2015

**Abstract:** In this work, the spatial and temporal variations of seismicity in northwestern Iran have been evaluated with a special focus on seismic precursors of the 11 August 2012 Mw 6.5 Varzeghan earthquake. The precursors are defined by the z-value test and the generalized fractal dimensions of earthquake epicenters. The investigation applies earthquakes that have occurred since 2006 in a region that includes the main shock and collected by the Iranian Seismological Center. In order to eliminate the effect of explosions in the processing, we removed the explosion from the used catalog by using the normalized ratio analysis of daytime to nighttime events. Having done the preprocessing procedures, we removed the events with magnitudes of less than 2.5. As a result of our analysis, a period of seismic quiescence has been identified, which started about 3 years before the Varzeghan main shock. In a nice coincidence with these results, significant changes have been observed in the generalized fractal dimensions and the related spectra prior to the occurrence of the Varzeghan earthquake. The changes indicate that the seismic activities of the studied area have had increasingly dense clustering in space since about mid-2009, which suggests the regional preparedness for the occurrence of the main quake. Furthermore, the analysis did not exhibit any significant seismic quiescence anomaly at the beginning of 2013.

**Key words:** Varzeghan earthquake, z-value, seismic quiescence, generalized fractal dimensions

## 1. Introduction

The northwest of the Iranian plateau displays a tectonic regime influenced by the motion of Arabia towards Eurasia. Tectonically, NW Iran is an intracontinental collision zone, and one of the main features in this region is the North Tabriz Fault accommodating several millimeters per year of right lateral strike slip motion, on the basis of GPS studies (e.g., Vernant et al., 2004; Djamour et al., 2011). NW Iran has been affected by seismic activity during historical and instrumental time periods. Some of these earthquakes are illustrated in Figure 1. An average recurrence period of at least 350 years for earthquakes with M > 7 is expected for the North Tabriz Fault (Hessami et al., 2003).

The 11 August 2012 Mw 6.5 Varzeghan earthquake (http://www.globalcmt.org/) was the latest catastrophic event in this region, which happened in the northeast of the North Tabriz Fault. Because of the poor quality of local construction, the Varzeghan quake led to invaluable costs of approximately 300 casualties and 3000 injuries along with extensive property damages. However, before the occurrence of this earthquake, no mapped faults were documented in its epicentral area. Joint inversion of teleseismic P and S wave data showed that the faulting in this event was strike-slip, right-lateral motion on an E–W plane. The centroid depth was assessed as 7 km (Copley et al., 2013), which is in the crustal seismogenic zone (Moradi et al., 2011).

This paper presents the results of an evaluation of earthquake potential before this quake in NW Iran and includes a study of 2 types of seismic precursors, i.e. seismic quiescence and temporal variations of fractal properties. The evaluation is based on some statistical characteristics of seismicity, namely the z-value (Wiemer and Wyss, 1994) and fractal dimension (Smalley et al., 1987). The findings are related to the evolution of seismic activities in this region. As mentioned by Polat et al. (2008), the results of such kinds of studies help to detect seismic anomalies before large earthquakes. Thus, they can provide useful information to assess the seismic hazard, not only in the study zone, but also in other active tectonic regions.

## 2. The area and data

The studied area is inside of a polygon bounded by (37°N, 44°E), (40°N, 44°E), (40°N, 49°E), and (37°N, 49°E) corner points in NW Iran (Figure 1).

* Correspondence: mehdi.zare.iran@gmail.com

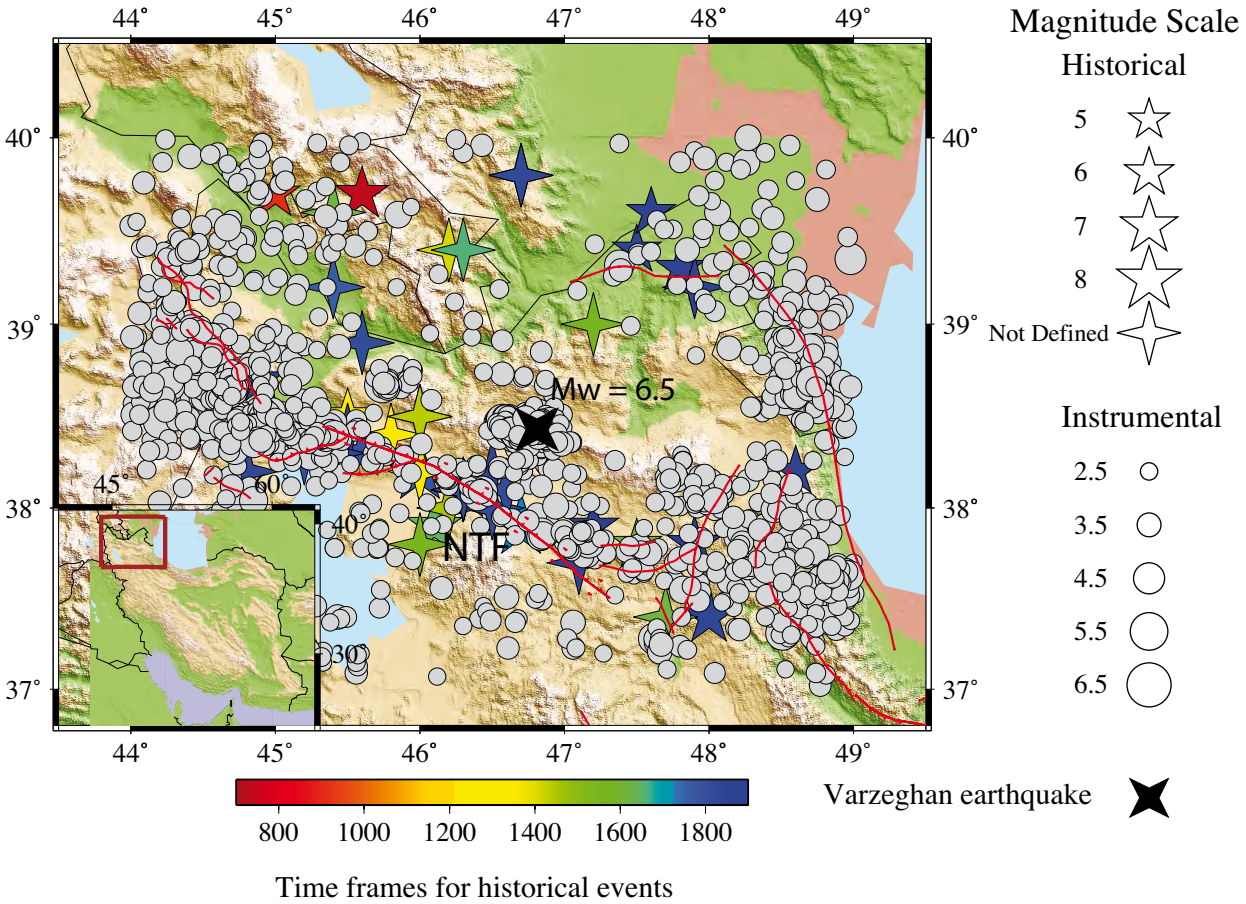


**Figure 1.** Historical and modern instrumental seismicity of 2006 to 2015 (M ≥ 2.5) in the Varzeghan-Azarbayjan zone: historical earthquakes (Ambraseys and Melville, 1982; Berberian, 1995), modern instrumental seismicity (IRSC), epicenter of the 2012 Varzeghan earthquake, and major faults are shown by stars, circles, black square, and solid lines respectively. NTF shows the North Tabriz Fault.

The applied data were extracted from the catalog of the Iranian Seismological Center (IRSC), which is available at http://irsc.ut.ac.ir/bulletin.php/. The studied area is approximately covered by the Tabriz local network. This network began in 1995. However, Rezapour (2005) discussed that the magnitude values for some years in the data set were not on the basis of a specific method. The present catalog lists events since 1 January 2006. In this period, the catalog was published in a consistent form based on the local magnitude scale (Mn) proposed by Rezapour (2005). This is an important advantage for a catalog over other composite catalogs to be almost homogenized and not to introduce magnitude shifts. Furthermore, this catalog is generally more accurate because it is based on a local seismic array.

We applied the catalog for the selected region in the period of 2006 to 2015. Up to the Varzeghan earthquake, the used data set contains about 3150 events shallower than 36 km with M ≥ 2. As the distribution of the magnitude of the data is mostly less than 4.5, the local magnitude, reported in the data set, was simply considered as the moment magnitude (Zare, 1999).

Figure 2 depicts the distribution of events in different hours of a day. Since there is a maximum range between 0700 and 1400 hours, the histogram suggests a significant contamination by explosions.

There are some studies in the literature for earthquake-explosion discrimination (e.g., Wiemer and Baer, 2000; Horasan et al., 2009; Yılmaz et al., 2013). In order to remove explosions, the normalized ratio (Rq) of daytime to nighttime events (Wiemer and Baer, 2000) is mapped based on seismic tool ZMAP 6.0. The 99th percentile was used as our significance threshold and N = 50 as the sample size for iterative removal of events from the data. After some iteration steps, 1114 daytime events, belonging to nodes with high Rq values, were excluded from the data

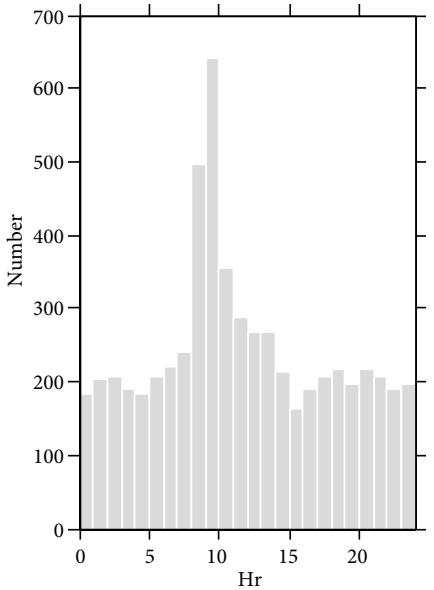


**Figure 2.** Histogram of events at different hours of a day for all events in the data set. Since there is a maximum range between 0700 and 1400 hours, the histogram suggests a significant contamination by explosions.

set (consisting of 5932 events). Approximately 90% of the total number of removed events had magnitudes of less than 2.3.

Figure 3a illustrates the Rq map based on the cleaned catalog. It is obvious that there are still some volumes with unacceptable values of Rq. After that, a magnitude bin of M = 2–2.3 was eliminated from the modified catalog and the ratio Rq was computed again. As can be seen in Figure 3b, approximately all the nodes have Rq ≤ 2.2 (or probability of occurrence Rq of less than 99%).

The magnitude of completeness (Mc) over time was then checked by the maximum curvature function (Wiemer and Wyss, 2000) using a sample size of 100 events. Figure 4a shows that Mc mostly varies between 2.4 and 2.5. However, there is a large fluctuation of Mc between 2012 and 2013 that is related to the 2012 Varzeghan earthquake sequence. This may be due to an aftershock sequence in which the small events may not be located (Öztürk, 2013). After the aforementioned treatments, in the cleaned catalog, we selected a total number of 2164 events having magnitudes of greater than 2.5. Figure 4b shows hourly distribution of the number of events for the final catalog. The histogram suggests a uniform distribution of events in different hours of a day, which is expected in reporting earthquakes.

To remove dependent events for detecting the precursory seismic quiescence, the catalog was declustered by the Reasenberg's algorithm (1985), as modified by Helmstetter et al. (2007). The error values of depth and epicenter location were changed to 10 and 7 km, respectively, and the rest of the parameters were considered as presented by Helmstetter et al. (2007). The declustering approach found 85 earthquake clusters (954 events out of 2164), and the obtained declustered catalog includes 1295 earthquakes.

In addition, Figure 5 indicates the distribution of earthquakes in time in the final catalog before and after declustering. The cumulative number curve of events for the declustered catalog is smoother than that of the raw catalog, showing that most of dependent events have been eliminated from the raw catalog by the declustering

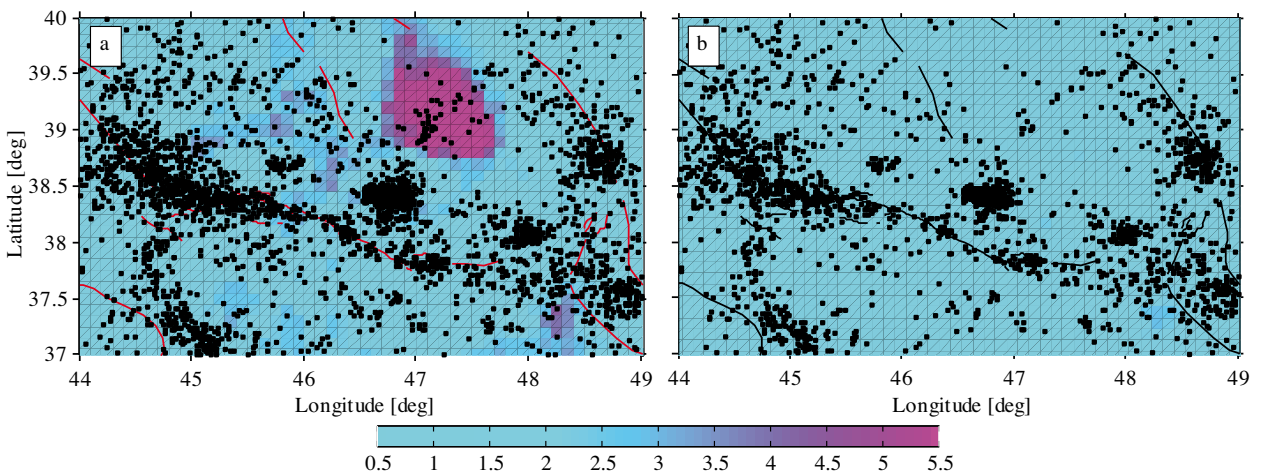


**Figure 3.** Quarry blast mapping: **a)** for the cleaned catalog, **b)** after removing events with M ≥ 2.3 within the cleaned catalog. In part b, approximately all the nodes have Rq ≤ 2.2 (or probability of occurrence Rq of less than 99%).

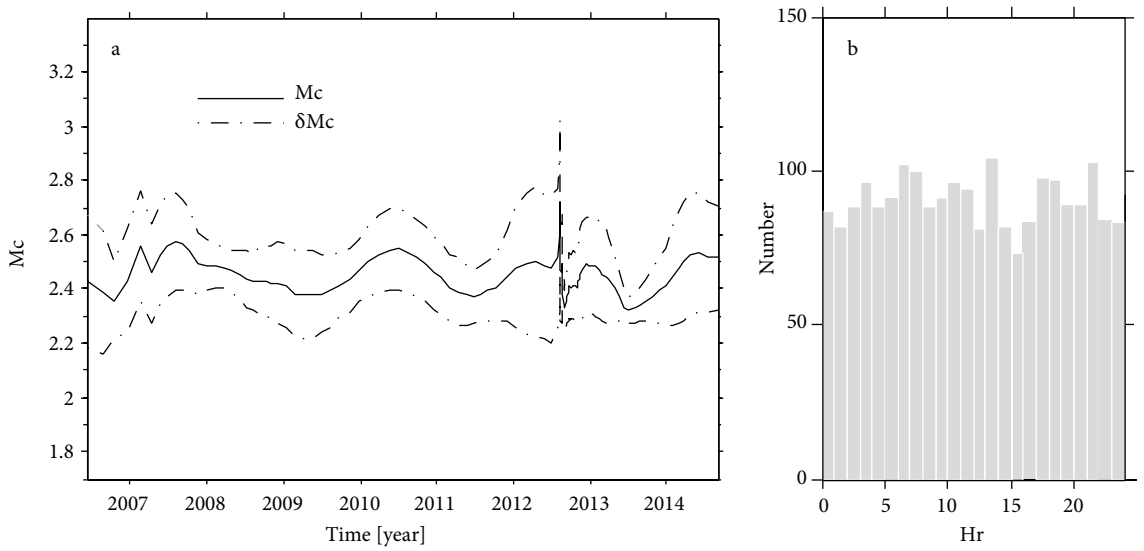


**Figure 4. a)** Magnitude completeness (Mc) as a function of time for the final catalog. This figure shows that Mc mostly varies between 2.4 and 2.5. **b)** Histogram of events in different hours of a day for the final catalog; the histogram suggests a uniform distribution of events in the different hours of a day.

process. However, there is a great seismicity change between 2012 and 2013, showing a relatively large number of aftershocks for the 2012 Varzeghan earthquake.

## 3. Methods

### 3.1. Seismic quiescence

Among premonitory phenomena preceding a main shock, seismic quiescence is one of the most considerable precursors. Many authors proposed this phenomenon for main shocks in a wide magnitude-range (e.g., M = 4.7 to 8 in Wyss and Habermann, 1988) as well as a wide duration range (e.g., 9 months for the Chi-chi quake (Wu and Chiao, 2006) and ~23 years for the Tohoku quake (Katsumata, 2011)).

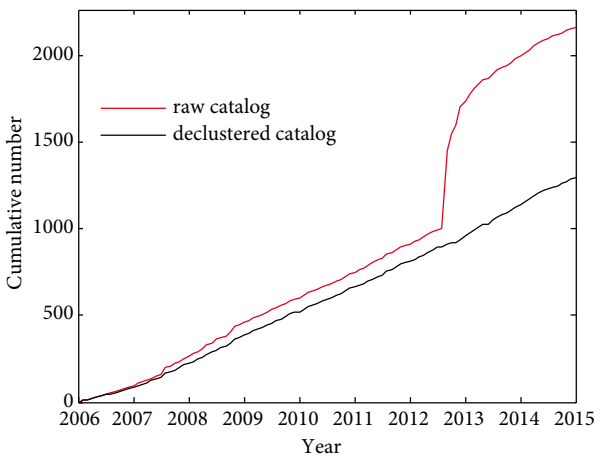


**Figure 5.** Temporal distribution of earthquakes in the final catalog before and after declustering. The curves indicate that most of the dependent events have been eliminated from the raw catalog by the declustering process.

Seismic quiescence is a significant reduction of the mean seismicity rate as compared to that corresponding to the background seismicity (Wyss and Habermann, 1988). The hypothesis of seismic quiescence can be considered as static (or elastic) stress change before large earthquakes.

In order to study seismicity rates, statistical methods must be applied (Matthews and Reasenberg, 1988). Accordingly, to detect quantitatively the time of maximum change, the z-value method has been applied using the LTA function, implemented in software package ZMAP 6.0 (Wiemer, 2001). This method has been extended to detect significant variations of seismicity rate within a catalog. The z-value is defined as follows (Wiemer and Wyss, 1994):

$$z = (R_1 - R_2) / \sqrt{(\sigma_1^2/n_1) + (\sigma_2^2/n_2)}, \quad (1)$$

where R is defined as the average of seismicity rate, σ is the standard deviation of seismicity rate, and n is the number of samples in the first and second periods, which are compared with each other. The LTA-function compares the seismicity rate in a time window (TW) with the overall average rate for a given area. The TW also moves at every possible point in time. For a more detailed definition of this function, we refer the reader to Öztürk and Bayrak (2012).

### 3.2. Multifractal analysis

Regional distributions of seismicity have often been considered as clustered. In other words, seismic patterns are not Poisson, even in declustered catalogs (e.g., De Natale and Zollo, 1986). Earthquakes are expected to happen within a range of magnitudes. The magnitude dependence of frequency usually satisfies the fractal scales. It can also be expected that the temporal behavior of seismicity influences the fractal clustering (Smalley et al., 1987). King (1983) suggested a fractal methodology for tectonics and Turcotte (1986a, 1986b) developed it.

Based on geological and seismological investigations, fault surfaces display mechanically heterogeneous properties at all scales (Candela et al., 2009). This kind of heterogeneity is related to differences of the material strength and the geometry in fault planes. In this way, seismic sequences, including foreshocks and aftershocks, are due to the faults' heterogeneities (Pechmann and Kanamori, 1982). Considering these heterogeneities, one is able to explain the fractal distributions and clustering of seismicity, which are quantified by means of fractal dimensions (Oncel and Wilson, 2006).

It is believed that a single fractal dimension is not enough to describe the heterogeneities. In other words, seismicity patterns and their variations through time and space are imprinted in the multifractals defined by generalized fractal dimensions $D_q$ of the seismicity. Using a multifractal approach (Hentschel and Procraccia, 1983) in some different seismic zones, several studies have considered the sequential changes of the heterogeneity in seismicity (e.g., Hirata and Imoto, 1991; Li et al., 1994; Teotia et al., 1997; Dimitriu et al., 2000; Sunmonu et al., 2001; Telesca et al., 2005; Teotia and Kumar, 2007, 2011). In addition, variations in the parameter q are useful to describe spatial-temporal patterns of clustering. Hence, changes in the seismicity behavior prior to the occurrence of strong seismic events can be inspected using the temporal behavior of $D_q$ (Li et al., 1994; Teotia and Kumar, 2007, 2011). Even for small data sets, multifractal analysis has been used for assessing generalized fractal dimension in several seismic zones, defined spatially as follows (Grassberger and Procaccia, 1983):

$$\log C_q(r) = D_q \log (r) \text{ , } (r \to 0), \tag{2}$$

$$C_q(r) = \lim_{r \to 0} \left\{ \frac{1}{N} \sum_{j=1}^{N} \left[ \frac{1}{N} \sum_{\substack{i=1 \\ i \neq j}}^{N} H\left(r - \left|X_i - X_j\right|\right) \right]^{(q-1)} \right\}^{1/(q-1)}, \tag{3}$$

where r is the scaling parameter of distance, N includes all the events occurring inside a region that is studied in a given time period, H(.) is the Heaviside step operator, $X_i$ and $X_j$ are respectively the epicentral locations of the i*th* and j*th* events, and $C_q(r)$ is the q*th* correlation integral. Similar to the spatial association, the temporal relation is defined by replacing r, $X_i$, and $X_j$ with the scaling parameter of time (t), i*th* occurrence time ($T_i$), and j*th* occurrence time ($T_j$), respectively, in Eqs. (2) and (3).

In this study, q varies between 2 and 15 in the generalized dimensions of seismicity distribution ($D_q$). The related measures of small q (e.g., q = 2) are associated with the regional scale clustering, whereas those of bigger q (e.g., q = 15) are related to local scale patterns of seismicity. As will be discussed later, the difference between $D_2$ and $D_{15}$ is a tool to measure the heterogeneity of fractal properties.

In order to estimate temporal changes of spatial $D_q$, similar to the study of Teotia and Kumar (2011), the data of subseries (subsets) obtained from all earthquake epicenters were used. There is no restriction on the number of data points within each subset and data points applied for a shift from one subset to another. Nevertheless, there is a trade-off between reliability and time resolution of fractal dimensions, in such a way that the larger the number of events is, the more reliable results are, but with less time resolution.

However, some authors have proposed several criteria to estimate the minimum number of samples ($N_{min}$) for evaluation of $D_q$ (e.g., Smith, 1988; Sornette et al., 1991). Smith (1988) suggested $N_{min}$ with a quality value Q ($0 \leq Q \leq 1$) as follows:

$$N_{min} \geq \left( \frac{(2-Q)R_{max}}{2(1-Q)R_{min}} \right)^M, \tag{4}$$

where $R_{min}$ and $R_{max}$ are minimum and maximum distances of the points and M is the integer part of $D_q$. If the distance of epicenters is used in this formula, $D_q$ is estimated to be less than 2, and therefore M equals 1.

## 4. Results

### 4.1. Changes in the seismicity rate

In order to calculate the seismic quiescence period, a set of TWs, i.e. 1.5, 2, 2.5, 3, 3.5, 4, 4.5, and 5 years, has been used in the analysis. Additionally, for continuous time coverage, a 28-day interval is considered for moving the TW. The z-value for the area is drawn as a map in Figure 6, in which the values have been computed for nodes with spacing of 0.1°. The neighbor earthquakes are taken as N = 200, by which the calculations are performed in each node. For a better comparison, the same color scale is used for all figures. In general, it can be said that TW and N are usually selected in a way that makes the quiescence signal more obvious (Öztürk and Bayrak, 2012). Due to the importance of the 2012 Varzeghan earthquake in this study, in all the maps in Figure 6, the z-values are depicted

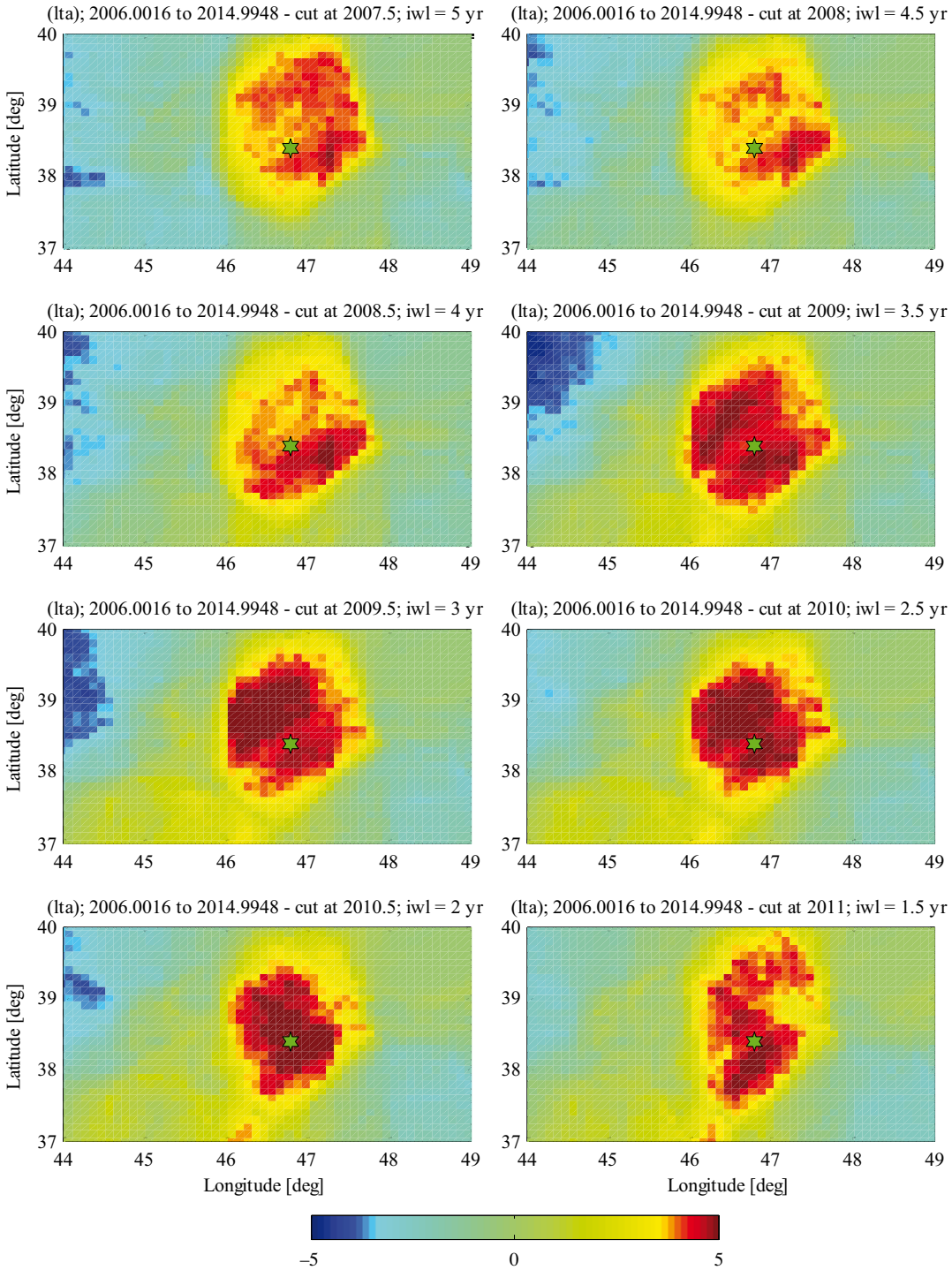


**Figure 6.** Mapped z-values for the area at the beginning of mid-2012 with a set of TWs, i.e. 1.5, 2, 2.5, 3, 3.5, 4, 4.5, and 5 years. Stars show epicenter location of the 2012 Varzeghan main shock.

for different TW values at the beginning of mid-2012 (before the occurrence of the Varzeghan earthquake).

In all the maps, an area with a significant quiescence anomaly can be observed. Nevertheless, as is seen, the anomaly with the 2-year TW is the strongest. This anomaly is visible in a wide area around the epicenter of the 2012

Varzeghan earthquake. As Öztürk and Bayrak (2012) stated, the z-value analysis applied in this study can help to ensure the reliability of the results.

In addition, for estimating the start-time of seismic quiescence, the values of the LTA function were calculated and plotted for earthquakes located around the epicenter of the 2012 Varzeghan earthquake (Figure 7). Since the anomaly is best revealed in Figure 6 with TW = 2 years, here this TW is located at every possible point in time, moving by 28 days. As it is seen, this function has a peak of z = 5.3 at 2010.2.

In order to illustrate the spatial distribution of z-values over time, the z-value map is presented for different cut-off times between 2007.5 and 2013 with a 2-year TW (Figure 8). As shown in this figure, no significant anomalies of seismic quiescence between 2006 and 2009 can be seen for anomalous area observed in Figure 6, but after 2009.5, a clear anomaly emerged there. No significant quiescence anomaly is observed between 2012.5 and 2013.

### 4.2. Multifractal values

In order to investigate multifractal values up to the 2012 Varzeghan earthquake, events that occurred in a circular area centered on the epicenter of the main shock were selected. Based on the average critical range of space related to the precursors of earthquakes with magnitudes of ~6 to 7 (Bowman et al., 1998), a radius of 150 km was supposed for the region affected by the seismicity associated with the Varzeghan earthquake.

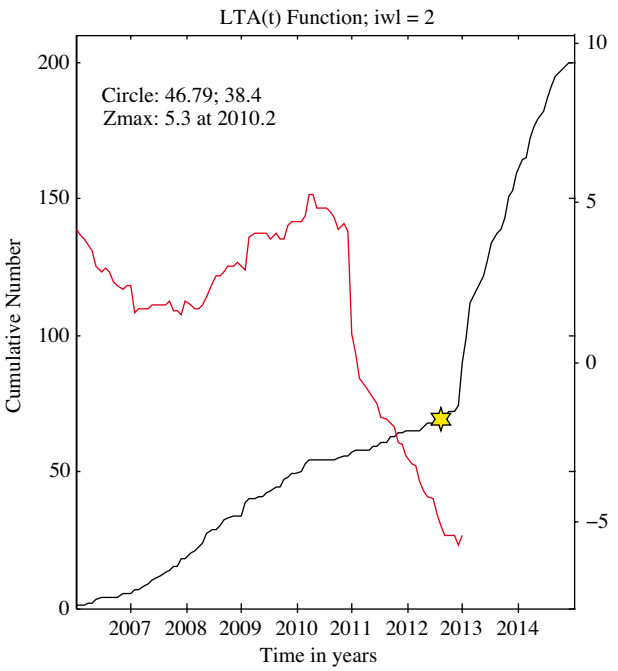


**Figure 7.** Cumulative number and the values of LTA function versus time for data located around the epicenter of the 2012 Varzeghan earthquake. The function has a peak of z = 5.3 at 2010.2. Star shows occurrence time of the 2012 Varzeghan earthquake.

Multifractal relationships within the data set are illustrated in Figure 9 until the Varzeghan quake. The fractal dimensions are estimated spatially in the linear region of the plot of versus (or of versus for the temporal generalized dimensions).

Similar to previous studies (e.g., Smalley et al., 1987; Tosi, 1998; Teotia and Kumar, 2011), the raw catalog is employed to estimate the fractal dimensions. On the basis of the data resolution in both time and space, with the time period of the data set (01/01/2006–11/08/2012) and the total number of data points (N = 351), the minimum time and space interval have been selected to be 1 min and 7 km, respectively.

Since random errors superimpose the earthquake locations, it is possible to define more than 1 straight line in the log–log plot of the correlation integral versus distance. It may suggest nonspecific results for the spatial generalized fractal dimension. This creates complexity in understanding which line is truly associated with earthquake clustering. Eliminating the data points ranging inside the estimated errors can solve the problem, without sacrificing the statistics of the calculations.

As mentioned above, error of the epicenter location of the selected data was estimated to be less than 7 km. Furthermore, there is an applied upper limit (due to edge effect) after which the correlation integral will cease to increase. Accordingly, distribution of seismicity in the data set obeys the spatial multifractal relation with $D_2(r)$ = 1.26 and $D_{15}(r)$ = 0.82 (Figure 9a) as well as the temporal relation with $D_2(t)$ = 0.93 and $D_{15}(t)$ = 0.72 (Figure 9b) before the occurrence of the Varzeghan quake.

### 4.3. Temporal variations of spatial fractal values

According to Smith (1988) and by assuming Q = 0.9, in the current study a value of ~80 was estimated as the minimum number of points ($N_{min}$) in each subset for calculating the fractal dimensions.

Here, the data set of the selected region, containing 530 earthquakes that occurred from 01/01/2006 to 13/08/2012, was divided into 10 subsets (S1–S10). Each subset consists of 80 events, and all of them have a coverage area of 30 events with each other (Table). All the subsets having the same number of earthquakes can avoid some effects of nonstationary signals in the data set (Teotia and Kumar, 2011).

The fractal dimensions $D_2(r)$ and $D_{15}(r)$ for all 10 subsets of the catalog are listed in the Table. Figure 10 also shows the temporal changes of these generalized fractal dimensions in all the subsets. The subset S7 contains the 2012 Varzeghan earthquake.

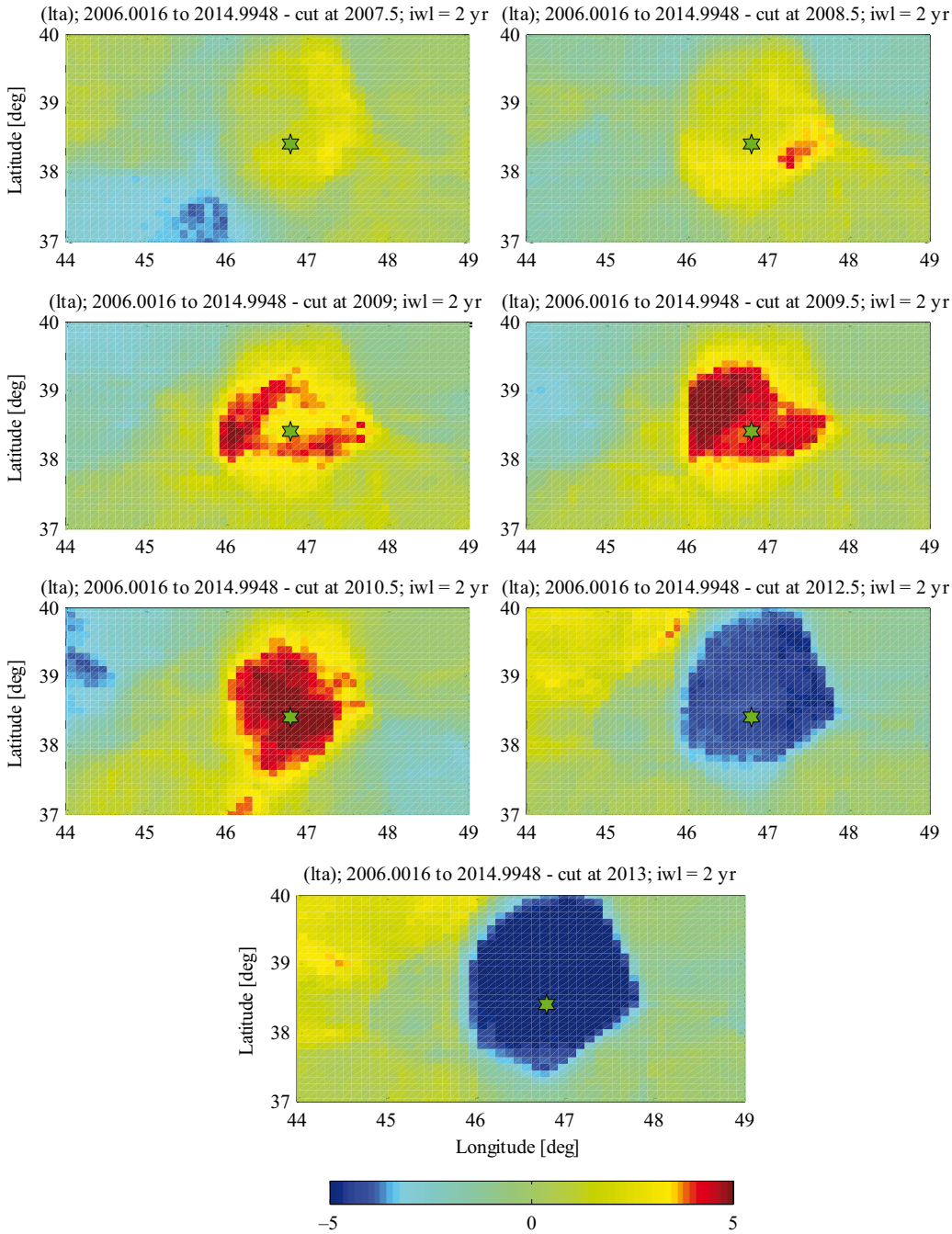


**Figure 8.** Spatial distribution of z-values for different cut-off times between mid-2007 and 2013. The length of the TW is chosen as 2 years. Stars show epicenter location of the 2012 Varzeghan earthquake.

## 5. Discussion

### 5.1. Seismicity rate

According to the investigation by Öztürk and Bayrak (2012) and taking into account the results in Figures 7 and 8, possibly seismic quiescence began in 2009 to 2010. In other words, the average length of the seismic quiescence period before the 2012 Varzeghan earthquake had been 3 years. Similar variations in the seismic behavior of the Iranian plateau were also documented ~3 years before the 26 December 2003 Bam, Iran, earthquake by means of z-test (Ashtari Jafari, 2012).

In recent years, some other similar studies have been done for different parts of Turkey, in the vicinity of our study area (e.g., Yılmaz et al., 2004; Öztürk et al., 2008). For

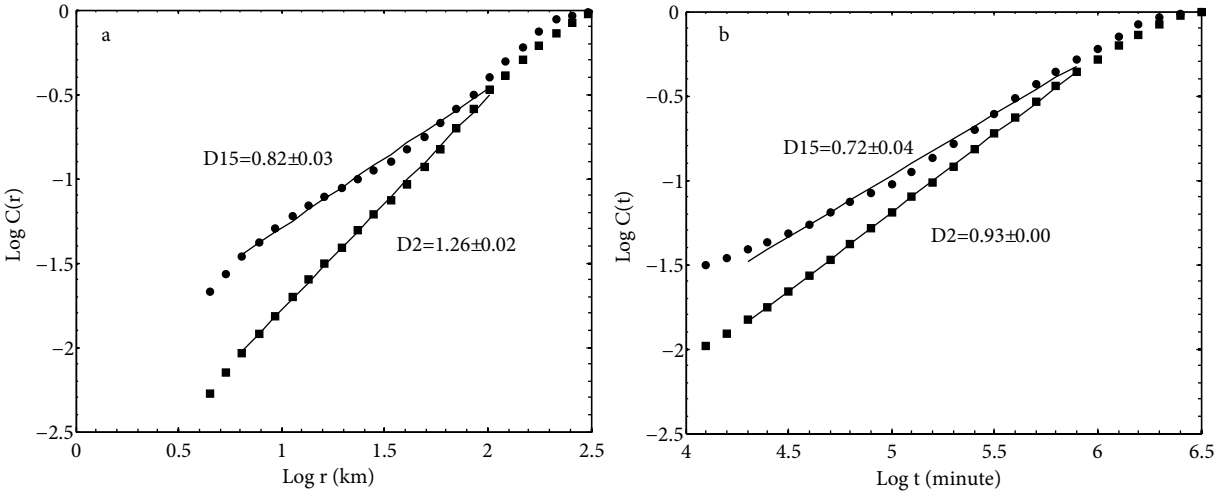


**Figure 9.** The plots illustrate the multifractal relationships observed in spatial and temporal analyses within data collected up to the occurrence of the 2012 Varzeghan earthquake. **a)** The linear region for space exists between ~7 and 100 km (i.e. between 0.85 and 2). **b)** The linear region in the temporal response extends from days to ~1.5 years (i.e. between 4.3 and 5.9).

example, in a statistical study, Yılmaz et al. (2004) assessed the seismic hazard in the North Anatolian Fault Zone, based on which Öztürk (2011) claimed that the average probability of earthquakes with magnitudes of greater than 5 in areas where significant quiescence anomalies emerged is more than 70%. Results of the present study are largely in accordance with their results and confirm the important role of the evaluation of seismic quiescence anomaly for the risk analysis of large earthquakes.

With regard to Figure 8, after the occurrence of the 2012 Varzeghan earthquake, no significant quiescence anomaly is seen in the study area up to 2013. Assuming an average length of ~3 years for the seismic quiet period in the study region, probably no earthquake with magnitude of greater than 6 (comparable to that of the 2012 Varzeghan earthquake) will occur up to 2016. However, due to the standard deviation of the average quiet period (Öztürk and Bayrak, 2012), which is ±1.5 years, the period predicted to be without occurrence of a major earthquake may be extended up to mid-2017.

### 5.2. Multifractal dimensions

The value of fractal dimension of q = 15, which is lower than that of q = 2 (Figure 9), indicates that the seismicity before the occurrence of the Varzeghan earthquake was dominated by clustering in local scales. The difference between $D_2(r)$ and $D_{15}(r)$ can help in assessing the behavior of complexity of a fault system. Because of differences between regional and local scales of fault complexity, and according to Oncel and Wilson (2006), the difference of 0.44 between $D_2(r)$ and $D_{15}(r)$, shown in Figure 9a, can

**Table.** The subset descriptions and fractal dimensions of the subsets.

| Subset name | Subset events | Time period | D2 | D15 |
|---|---|---|---|---|
| S1 | 1–80 | 2006/01/01–2007/07/18 | 1.36 | 1.16 |
| S2 | 51–130 | 2007/03/31–2008/04/07 | 1.43 | 1.17 |
| S3 | 101–180 | 2007/11/16–2008/01/12 | 1.38 | 1.14 |
| S4 | 151–230 | 2008/06/26–2010/01/04 | 1.26 | 0.83 |
| S5 | 201–280 | 2009/04/18–2011/01/29 | 1.13 | 0.94 |
| S6 | 251–330 | 2010/06/02–2012/02/25 | 0.95 | 0.62 |
| S7 | 301–380 | 2011/06/16–2012/08/11 | 0.73 | 0.43 |
| S8 | 351–430 | 2012/07/15–2012/08/11 | 0.67 | 0.45 |
| S9 | 401–480 | 2012/08/11–2012/08/12 | 0.46 | 0.29 |
| S10 | 451–530 | 2012/08/12–2012/08/13 | 0.54 | 0.34 |

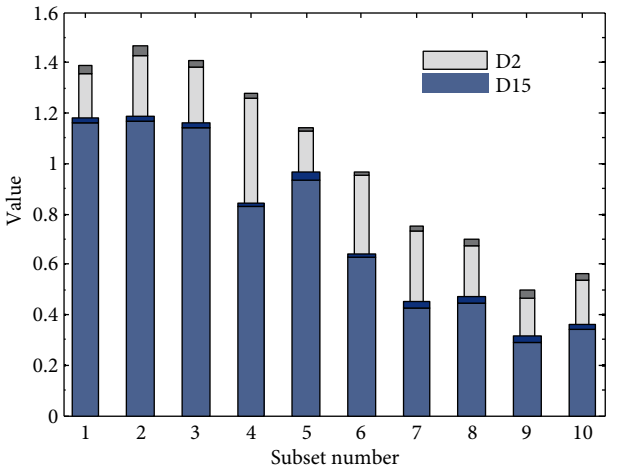


**Figure 10.** Bar graphs of the generalized fractal dimensions $D_q(r)$ (q = 2 and 15) in subsets S1–S10. The graphs display the temporal variations of the generalized fractal dimensions in the studied period. Darkened regions at tops of bars show the upper ranges of confidence intervals of the values. Subset S7 contains the Varzeghan 2012 earthquake. This figure illustrates the decrease in the fractal dimensions before the main shock.

reflect the existence of significant fractal heterogeneities in the pattern of the seismicity. Moreover, it is inferred that the area had had high spatial complexity before the main shock.

The differences between $D_2(t)$ and $D_{15}(t)$ also assess the variations of complexity of seismicity over time (Oncel and Wilson, 2006). In the current case, a small value of $\Delta D(t)$ (i.e. 0.21) can imply that high spatial complexity varied little or maybe gradually over the time period leading up to the 2012 Varzeghan earthquake.

Based on the work of Kagan and Jackson (1991) on seismic clustering for interpreting the results of $D_2(t)$, the following criteria can be used:

1) Temporal behavior of seismicity may be divided into long-term (with $D_2(t)$ = 0.8–1) and short-term clustering (with $D_2(t)$ ~0.5).

2) Highly clustered seismicity is mainly attributed to a sequence of earthquakes (short-term foreshock, main shock, and aftershock activity), whereas weakly clustered seismicity is mainly associated with main shocks.

3) Seismicity distribution in time is periodic with $D_2(t)$ ~0.5, quasiperiodic with $D_2(t)$ ~0.75, and random with $D_2(t)$ ~1.

Accordingly, the results reflect that the seismic distribution of the Varzeghan-Azarbayjan area was random through time. In other words, it was close to a Poisson process. In addition, the lack of strong events in the area for the time duration of the analysis indicates that earthquake clustering in this area is not effectively influenced by aftershock and foreshock activities.

### 5.3. Temporal changes of spatial fractal properties

According to Figure 10, it is evident that the period of the increase in clustering (lowering value of fractal dimensions) was before the occurrence of the 2012 Varzeghan quake. A similar observation was also reported by Teotia and Kumar (2011) for the occurrence of the October 2005 Muzaffrabad-Kashmir, India, earthquake.

Additionally, for checking the robustness of the results, a set of different numbers of points (N) for each subset (i.e. 80, 90, 100, 110, 120, 130, 140, and 150) and for the shifting intervals (i.e. 30, 50, and 70) was used (Figure 11). The mean and standard deviation of the obtained values are presented in Figure 11. According to Smith (1988), in the present study N = 80 and 150 are estimated as the minimum number of points ($N_{min}$) in a subset at the quality levels of 0.9 and 0.95, respectively. In Figures 11a and 11b, the values of $D_q$ estimated for the subsets are assigned to the center of the corresponding time intervals. In concert with the results presented in Figure 10, a period of low values of $D_2$ (Figure 11a) and $D_{15}$ (Figure 11b) is evident since about mid-2009 to the occurrence time of the Varzeghan earthquake for all the sets of the parameters. Therefore, the interpretations of the decrease in the fractal dimensions prior to the main shock will be strengthened more as the sensitivity test rejects the dependence of the results on the inputs.

$D_q$-q spectra (Figure 12) are also plotted to show the clustering in the zone of preparation for the Varzeghan earthquake. This confirms the decrease in fractal dimensions before the main shock.

Subset S2 (Figure 12) is situated ~5 years prior to the occurrence of the Varzeghan earthquake, and its relatively large values of $D_q$ imply that the seismicity relevant to background activities can be observed in this subset. Subset S6 was laid ~1.5 years before the main quake, and moderate values of its corresponding $D_q$ indicate that seismicity of subset S6 is going to present clustering and arrangement of the main shock. Low values of $D_q$ for subset S7, including the Varzeghan earthquake, show that seismicity of this subset is highly localized in space. Subsets S9 and S10 consist mostly of highly clustered seismic activities causing very small values of fractal dimensions. In fact, this stage introduces a new seismic clustering caused by aftershocks.

The fractal dimensions $D_2(r)$ and $D_{15}(r)$ not only can indicate the amount of earthquake clustering for a zone, but also characterize the stress state over it. Hence, it can be suggested that the decline of these dimensions before the Varzeghan earthquake is possibly because of effective stress variations.

Overall, the regular reduction of the spatial fractal dimensions since ~2009 is thought to be due to the decrease in the fault complexity, an activation of seismic

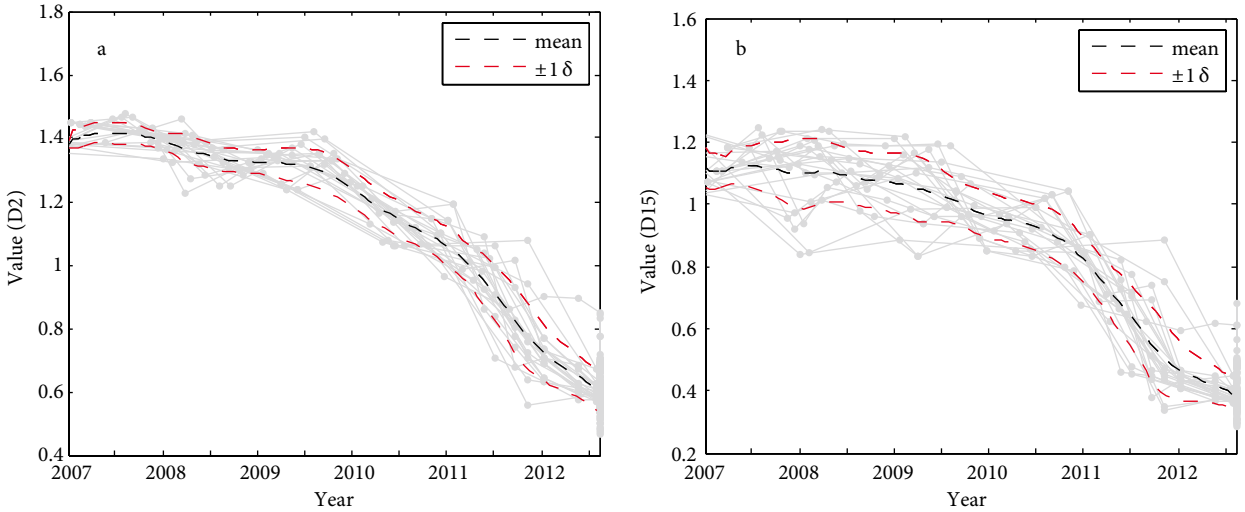


**Figure 11.** Sensitivity of $D_q$ to different numbers of points (N) in each subset (i.e. 80, 90, 100, 110, 120, 130, 140, and 150) and to shifting intervals (i.e. 30, 50, and 70). **a)** $D_2$, **b)** $D_{15}$. According to Smith (1988), N = 80 and 150 are estimated to be the minimum number of points ($N_{min}$) in a subset for Q = 0.9 and 0.95, respectively. The results for the sets of the input parameters are shown by solid lines. The corresponding means and error bars are both shown by dashed lines. All of the results illustrate the decrease in the fractal dimensions before the 2012 Varzeghan main shock.

clustering in the area, and regional preparedness before the occurrence of the Varzeghan main shock. Approximately 99% of the total number of earthquakes that occurred in this period had magnitudes of less than 3.5. Furthermore, the anomaly of the seismic quiescence is in good agreement with the reduction in the fault complexity.

As Oncel and Wilson (2002) illustrated, it can be interpreted that during the period of seismic quiescence, the reduced complexity in the active fault network accommodates seismicity of smaller magnitudes along the fault planes with relatively smaller surface areas. With respect to our results, it can be inferred that during the quiet period, only a small part of stress in this region had been released through small-sized earthquakes. Additionally, the major part of stress probably caused the occurrence of the main shock and its interrelated earthquakes. This can be evidenced by a relatively large number of aftershocks related to the 2012 Varzeghan earthquake.

As mentioned in Sections 5.1 and 5.3, the observed anomalies of seismic quiescence and fractal dimensions are largely in accordance with those of some other similar studies carried out for some active tectonic regions. They can provide an opportunity to get an insight into the temporal-spatial dynamics of seismicity. Thus, such kinds of seismic precursors could contribute to the forecasting of future strong earthquakes. From this point of view, our results (Sections 4.1 and 5.1) suggest a period without any major earthquakes up to mid-2017 for the studied area.

However, it is obvious that there may be precursory anomalies unrelated to the main shocks, called false

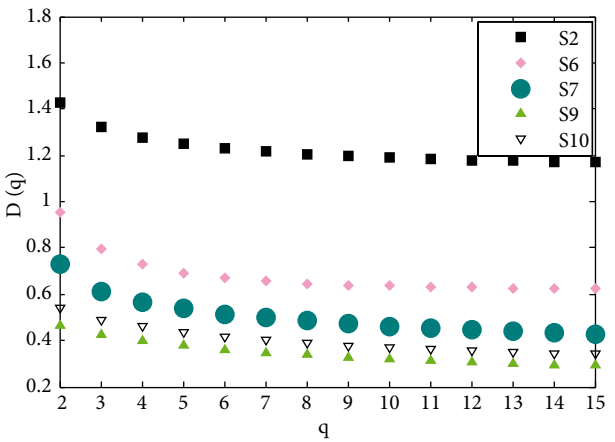


**Figure 12.** $D_q$-q spectra of subsets S2, S6, S7, S9, and S10. Corresponding values of subset S7, which contains the Varzeghan Mw = 6.5 earthquake, are highlighted by filled circles. This figure illustrates the decrease in the fractal dimensions before the main shock.

alarms, and/or main shocks with missed alarms. This means that precursors such as seismic quiescence are not necessarily associated with a forthcoming main shock and vice versa. Hence, for the utilization of such a precursor for risk management, measurements of other short-term, mid-term, and long-term precursors should be made concurrently.

**Acknowledgments**
The authors would like to acknowledge International Institute of Earthquake Engineering and Seismology (IIEES) for its help in providing research documents and methodological aspects of the job and Iranian Seismological Center (IRSC) for providing earthquake database via internet. We would like to thank numerous colleagues, namely Dr H Zafarani, Dr A Ansari, E Noroozinejad, M Mahmudabadi, M Farrokhi, and M Ahmadi-Borji, for sharing their points of view on the manuscript. We are grateful to Dr O Polat and two anonymous reviewers for their valuable comments. We also thank S Wiemer for use of his software, ZMAP 6.0.

## References

Ambraseys NN, Melville CP (1982). A History of Persian Earthquakes. 1st ed. Cambridge, UK: Cambridge University Press.

Ashtari Jafari M (2012). Seismicity anomalies of the 2003 Bam, Iran earthquake. J Asian Earth Sci 56: 212–217.

Berberian M (1995). Natural Hazards and the First Earthquake Catalogue of Iran, Historical Hazards in Iran Prior to 1900. 1st ed. Tehran, Iran: IIEES.

Bowman DD, Ouillon G, Sammis CG, Sornette A, Sornette D (1998). An observational test of the critical earthquake concept. J Geophys Res 103: 24359–24372.

Candela T, Renard F, Bouchon M, Brouste A, Marsan D, Schmittbuhl J, Voisin C (2009). Characterization of fault roughness at various scales: implications of three-dimensional high resolution topography measurements. Pure Appl Geophys 166: 1817–1851.

Copley A, Faridi M, Ghorashi M, Hollingsworth J, Jackson J, Nazari H, Oveisi B, Talebian M (2013). The 2012 August 11 Ahar earthquakes: consequences for tectonics and earthquake hazard in the Turkish–Iranian Plateau. Geophys J Int 196: 15–21.

De Natale G, Zollo A (1986). Statistical analysis and clustering features of the Phlegraean Fields earthquake sequence (May 1983-May 1984). B Seismol Soc Am 76: 801–814.

Dimitriu PP, Scordilis EM, Karacostas VG (2000). Multifractal analysis of the Arnea, Greece seismicity with potential implications for earthquake prediction. Nat Hazards 21: 277–295.

Djamour Y, Vernant P, Nankali HR, Tavakoli F (2011). NW Iran-eastern Turkey present-day kinematics: results from the Iranian permanent GPS network. Earth Planet Sc Lett 307: 27–34.

Grassberger P, Procraccia I (1983). Measuring the strangeness of strange attractors. Physica D 9: 189–208.

Helmstetter A, Kagan YY, Jackson DD (2007). High resolution, time-independent grid-based forecast for M ≥ 5 earthquakes in California. Seismol Res Lett 78: 78–86.

Hentschel HGE, Procraccia I (1983). The infinite number of generalized dimensions of fractals and strange attractors. Physica D 8: 435–444.

Hessami K, Pantosti D, Tabassi H, Shabanian E, Abbassi MR, Feghhi K, Solaymani S (2003). Paleoearthquakes and slip rates of the North Tabriz Fault, NW Iran: preliminary results. Ann Geophys 46: 903–915.

Hirata T, Imoto M (1991). Multifractal analysis of spatial distribution of micro earthquakes in the Kanto region. Geophys J Int 107: 155–162.

Horasan G, Boztepe-Güney A, Küsmezer A, Bekler F, Öğütçü Z, Musaoğlu N (2009). Contamination of seismicity catalogs by quarry blasts: an example from Istanbul and its vicinity, northwestern Turkey. J Asian Earth Sci 34: 90–99.

Kagan YY, Jackson DD (1991). Long-term earthquake clustering. Geophys J Int 104: 117–133.

Katsumata K (2011). A long-term seismic quiescence started 23 years before the 2011 off the Pacific coast of Tohoku Earthquake (M = 9.0). Earth Planets Space 63: 709–712.

King G (1983). The accommodation of large strains in the upper lithosphere of the earth and other solids by self-similar fault systems: the geometrical origin of b-value. Pure Appl Geophys 121: 761–815.

Li D, Zhaobi Z, Binghong W (1994). Research into the multifractal of earthquake spatial distribution. Tectonophysics 223: 91–97.

Matthews MV, Reasenberg P (1988). Statistical methods for investigating quiescence and other temporal seismicity patterns. Pure Appl Geophys 126: 357–372.

Moradi A, Hatzfeld D, Tatar M (2011). Microseismicity and seismotectonics of the North Tabriz fault (Iran). Tectonophysics 506: 22–30.

Oncel AO, Wilson T (2002). Space-time correlations of seismotectonic parameters: examples from Japan and from Turkey preceding the Izmit earthquake. B Seismol Soc Am 92: 339–349.

Oncel AO, Wilson T (2006). Evaluation of earthquake potential along the Northern Anatolian Fault Zone in the Marmara Sea using comparisons of GPS strain and seismotectonic parameters. Tectonophysics 418: 215–218.

Öztürk S (2011). Characteristics of seismic activity in the Western, Central and Eastern parts of the North Anatolian Fault Zone, Turkey: temporal and spatial analysis. Acta Geophys 59: 209–238.

Öztürk S (2013). A statistical assessment of current seismic quiescence along the North Anatolian Fault Zone: earthquake precursors. Austrian J Earth Sci 106: 4–17.

Öztürk S, Bayrak Y (2012). Spatial variations of precursory seismic quiescence observed in recent years in the eastern part of Turkey. Acta Geophys 60: 92–118.

Öztürk S, Bayrak Y, Çinar H, Koravos GC, Tsapanos TM (2008). A quantitative appraisal of earthquake hazard parameters computed from Gumbel I method for different regions in and around Turkey. Nat Hazards 47: 471–495.

Pechmann JC, Kanamori H (1982). Waveforms and spectra of preshocks and aftershocks of the 1979 Imperial Valley, California, earthquake: evidence for fault heterogeneity? J Geophys Res 87: 10579–10597.

Polat O, Gök E, Yılmaz D (2008). Earthquake hazard of the Aegean extension region (West Turkey). Turk J Earth Sci 17: 593–614.

Reasenberg P (1985). Second order moment of central California seismicity 1969–1982. J Geophys Res 90: 5479–5495.

Rezapour M (2005). Magnitude scale in the Tabriz seismic network. J Earth Space Phys 31: 13–21.

Smalley RF Jr, Chatelian JL, Turcotte DL, Prevot A (1987). A fractal approach to the clustering of earthquakes: applications to the seismicity of New Hebrides. B Seismol Soc Am 77: 1368–1381.

Smith LA (1988). Intrinsic limits on dimension calculations. Phys Lett A 133: 283–288.

Sornette A, Dubois J, Cheminde JL, Sornette D (1991). Are sequences of volcanic eruptions deterministically chaotic? J Geophys Res 96: 11931–11945.

Sunmonu LA, Dimri VP, Prakash MR, Bansal AR (2001). Multifractal approach to the time series of M ≥ 7.0 earthquake in Himalayan region and its vicinity during 1895–1995. J Geol Soc India 58: 163–169.

Telesca L, Lapenna V, Macchiato M (2005). Multifractal fluctuations in seismic inter spike series. Physica A 354: 629–640.

Teotia SS, Khattri KN, Roy PK (1997). Multifractal analysis of seismicity of the Himalayan region. Curr Sci India 73: 359–366.

Teotia SS, Kumar D (2007). The great Sumatra-Andaman earthquake of 26 December 2004 was predictable even from seismicity data of mb ≥ 4.5: a lesson to learn from nature. Indian J Mar Sci 36: 122–127.

Teotia SS, Kumar D (2011). Role of multifractal analysis in understanding the preparation zone for large size earthquake in the North-Western Himalaya region. Nonlinear Proc Geoph 18: 111–118.

Tosi P (1998). Seismogenic structure behavior revealed by spatial clustering of seismicity in the Umbria-Marche region (Central Italy). Ann Geophys 41: 215–224.

Turcotte DL (1986a). Fractals and fragmentation. J Geophys Res 91: 1921–1926.

Turcotte DL (1986b). A fractal model for crustal deformation. Tectonophysics 132: 261–269.

Vernant P, Nilforoushan F, Hatzfeld D, Abbassi MR, Vigny C, Masson F, Nankali H, Martinod J, Ashtiani A, Bayer R et al. (2004). Present-day crustal deformation and plate kinematics in the Middle East constrained by GPS measurements in Iran and northern Oman. Geophys J Int 157: 381–398.

Wiemer S (2001). A software package to analyze seismicity: ZMAP. Seismol Res Lett 72: 373–382.

Wiemer S, Baer M (2000). Mapping and removing quarry blast events from seismicity catalogs, short notes. B Seismol Soc Am 90: 525–530.

Wiemer S, Wyss M (1994). Seismic quiescence before the Landers (M=7.5) and Big Bear (6.5) 1992 earthquakes. B Seismol Soc Am 84: 900–916.

Wiemer S, Wyss M (2000). Minimum magnitude of completeness in earthquake catalogs: examples form Alaska, the western United States, and Japan. B Seismol Soc Am 90: 859–969.

Wu YM, Chiao LY (2006). Seismic quiescence before the 1999 ChiChi, Taiwan Mw7.6 earthquake. B Seismol Soc Am 96: 321–327.

Wyss M, Habermann RE (1988). Precursory seismic quiescence. Pure Appl Geophys 126: 319–332.

Yılmaz Ş, Bayrak Y, Çınar H (2013). Discrimination of earthquakes and quarry blasts in the eastern Black Sea region of Turkey. J Seismol 17: 721–734.

Yılmaz V, Erişoğlu M, Çelik HE (2004). Probabilistic prediction of the next earthquake in the NAFZ (North Anatolian Fault Zone), Turkey. Doğuş Üniversitesi Dergisi 5: 243–250.

Zare M (1999). Contribution a l'etdue des mouvements forts en Iran; du catalogie aux lois d'attenuation. PhD, Universite Joseph Fourier, Grenoble, France (in French).